Towards an enhanced coupling between the Er ions and Si nanoclusters

L. Khomenkova, F. Gourbilleau, J. Cardin, R. Rizk

Towards an enhanced coupling between the Er ions and Si nanoclusters

L. Khomenkova *, F. Gourbilleau, J. Cardin, R. Rizk

CIMAP, UMR CNRS/CEA/ENSICAEN/ Université de Caen, 6 Bd Maréchal Juin, 14050 Caen Cedex 4, France

A B S T R A C T

The reactive magnetron co-sputtering of two confocal SiO_2 and Er_2O_3 cathodes in argon–hydrogen plasma was used to deposit Er-doped Si-rich-SiO_2 layers. The effects of deposition conditions (such as hydrogen rate and substrate temperature) and annealing treatment (temperature and time) on the structural, compositional and photoluminescence (PL) properties of the layers were examined. An enhancement was observed of both Er^{3+} PL emission and Er^{3+} lifetime at 1.54 μm in comparison with their counterparts for the best samples reported so far. It was shown that a lifetime as high as 9 ms can be reached, with comparable PL intensities for resonant and non-resonant excitation lines. The effective cross-section and the fraction of Er ions coupled to Si clusters are analyzed.

Keywords:
Reactive magnetron sputtering
Si nanocluster
Erbium
Photoluminescence
Lifetime

1. Introduction

Erbium-doped materials are under an intense research because of their potential optoelectronic and photonic applications due to sharp photoluminescence (PL) at 1.54 μm. Such emission comes from the $^4I_{13/2}$–$^4I_{15/2}$ transition in the internal 4f-shell of the Er^{3+} ions and corresponds to the minimum absorption of the silica-based optical fibres.

During the last years, numerous Si-based materials have been investigated as a host for Er ions, like crystalline silicon (c-Si) and sub-stoichiometric SiO_x ($1<x<2$) up to SiO_2 [1]. In c-Si, a strong temperature quenching of the Er^{3+} PL was observed and attributed to Auger de-excitation and energy back-transfer processes [2], while in Er-doped-SiO_2 materials the de-excitation processes of the Er^{3+} PL are practically absent but suffers from the low excitation cross-section of Er, σ_{eff} ($\sim 10^{-21}$ cm^2) [3] that requests pumping by expensive high-power lasers.

However, the sub-stoichiometric SiO_x or Si-rich silicon oxide (SRSO) appears highly interesting as host material, since it leads to nearly two orders of magnitude enhancement of the Er^{3+} PL, compared to Er-doped SiO_2 [4–9]. This effect was attributed to the presence of Si nanoclusters, Si-nc, and to a strong coupling between them and Er^{3+} ions [5–10]. Then the increase of σ_{eff} up to 10^{-16} cm^{-2} [11] was demonstrated, corresponding to the absorption cross-section of Si-nc [12]. The sensitizing role is independent of the crystalline or amorphous nature of Si-nc [13,14], and the energy transfer from Si-nc to Er^{3+} ions is highly dependent on their separating distance, which should be less than 0.5 nm [15,16]. Such a distance dependence is considered to be responsible for the few percentage of Er coupled to Si-nc [8,17].

Recently, our team has developed a novel approach for the fabrication of Er-SRSO layers by the reactive co-sputtering of two confocal cathodes of Er_2O_3 and SiO_2, instead of the reactive sputtering of a single SiO_2 target topped by Er_2O_3 chips, as described in Refs. [14,16–18]. Moreover, the deposition was made on a rotating substrate, leading to a better homogeneity of both growth and composition of the layers. The content of Er and Si excess can be finely and independently tuned through the monitoring of the RF power applied on each cathode, the hydrogen rate r_H and the substrate temperature T_S.

2. Experimental

The layers investigated have been fabricated by the reactive magnetron co-sputtering of 2 in confocal pure SiO_2 and Er_2O_3 cathodes under argon–hydrogen mixture onto 4 in silicon p-type substrates. The incorporation of Si excess in the layers was due to the ability of hydrogen to reduce reactively the oxygen species present in plasma, as previously described in Ref. [19]. The control of the Si excess in the layers was made through the variation of the hydrogen rate $r_H = F_{H_2}/(F_{H_2} + F_{Ar})$, where F_{H_2} and F_{Ar} are the values of gas flow for hydrogen and argon, respectively. The total flow of both gases was kept constant at 10 sccm, while the variation of F_{H_2} from 2 to 8 sccm allows modifying the r_H value in

* Corresponding author. Tel.: +33 231452656; fax: +33 231452660.
E-mail address: larysa.khomenkova@ensicaen.fr (L. Khomenkova).

the range 20–80%. The total pressure in the chamber and the power density applied onto SiO_2 and Er_2O_3 cathodes were fixed at 3 mTorr, 7.4 and 0.74 W/cm^2, respectively, while the substrate temperature (T_S) was varied between 50 and 200 °C. All the layers were annealed at 700–900 °C during 2–60 min in nitrogen flow.

The Si excess and disorder in the layers were studied by means of the Fourier transform infra red (FTIR) absorption technique. FTIR spectra were recorded under normal and Brewster incident angle (65°) in the range 500–4000 cm^{-1} using a Nicolet Nexus spectrometer.

Energy-dispersive spectroscopy (EDS) was performed to check the composition of the layers, allowing the estimate of the Er content to about $(3–4)\times10^{20}$ cm^{-3} for all layers investigated. The thickness and the refractive index of the layers were determined by spectroscopic ellipsometry and/or m-lines methods.

PL spectra of SRSO-Er layers were detected at room temperature using a Jobin Yvon 1 m single grating monochromator and Northcoast germanium detector cooled with liquid nitrogen. PL was excited by means of Ar$^+$-laser operating at either 476 nm (non-resonant) or 488 nm (resonant) lines. The pumping photon flux was varied in the range 1×10^{16}–4×10^{20} ph/cm^2 s. For the sake of comparison, all the PL spectra were normalized on the excited volume after being recorded with a photon flux of 4×10^{18} ph/cm^2 s for both excitations. The lifetime study was performed with a flux of 1×10^{16} ph/cm^2 s.

3. Results and discussion

The variation of the processing conditions (growth and thermal treatment) was performed with the aim of optimizing the Er PL and an enhancement of the fraction of coupled Er^{3+} ions.

3.1. Effect of hydrogen rate

The typical effect of r_H on the PL properties of SRSO-Er is demonstrated for the layer deposited at $T_S = 100$ °C and annealed at 900 °C during 60 min (Fig. 1, curve 1). The PL intensity improves with the first stages of r_H increase, reaches a maximum for r_H~55%, before decreasing when r_H is further increased up to 80%. This contrasts with the observed continuing decrease of Er^{3+} lifetime (Fig. 1, curve 2). Such behaviours of PL parameters could be explained by the variation of excess Si, as well as by the change of the proportion of coupled Er.

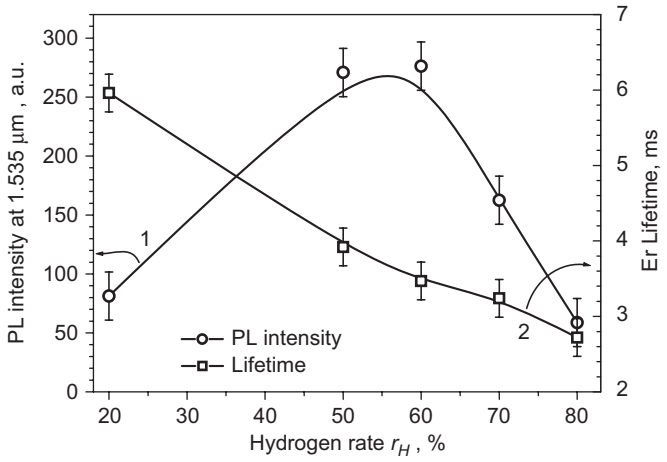

Fig. 1. Dependence of Er^{3+} PL intensity (curve 1) and lifetime (curve 2) of SRSO-Er layers deposited at $T_S = 100$ °C on the hydrogen rate r_H. The measurements were made by using the non-resonant excitation line (476 nm).

The Si excess induced by r_H variation was estimated from the evolution of the FTIR spectra recorded at normal incidence (not shown) following the method described in Ref. [20]. Briefly summarized, this method is based on a linear relation between the shift on the TO_3 peak position for a sub-stoichiometric SiO_x ($1<x<2$) matrix, with respect to that of SiO_2, and the stoichiometric coefficient x. The highest Si excess was found around 10 at%, while the Si excess for the layers showing the highest PL has been estimated to be about 5 at%. These results were also confirmed by EDS measurements. The increase in the excess Si is expected to enhance the density and/or the average size of Si-nc, which are still amorphous and then hardly observable by transmission electron microscopy [21].

Consequently, the increase in the PL intensity, when r_H is increased from 20% to 55%, could be explained by the increasing density of Si-nc sensitizers, which, in turn, improves the fraction of coupled Er. However, for higher values of r_H ($r_H>55\%$) that induce more and more Si excess, one expects some increase in the average size of Si-nc at the expense of their density and their coupling with Er ions. This might explain the observed PL decrease for $r_H>55\%$, even though the concomitant increasing disorder can also contribute to such a behaviour. The increase of the disorder with the Si excess is confirmed by the evolution of the TO_4–LO_4 doublet of the FTIR spectra recorded at Brewster incidence (not shown), and is considered responsible for the gradual decrease of the Er^{3+} lifetime shown in Fig. 1. It is worth noting that the highest PL intensity for this series corresponds to a lifetime of 3.5–4 ms.

3.2. Effect of the temperature of substrate

The analysis of the effect of T_S on the Er^{3+} PL properties of SRSO-Er layers is presented for the samples showing the best PL features in the previous section (r_H effect). Fig. 2 shows the evolution of both Er^{3+} PL and lifetime against T_S for the layers deposited at $r_H = 60\%$ and then annealed at 900 °C during 60 min. Both PL intensity and lifetime demonstrate behaviours similar to their counterparts for the r_H effect (Fig. 1). After a first increase, the PL reaches a maximum for $T_S = 80$–100 °C, before decreasing for higher values of T_S. In contrast, the lifetime shows a smooth continuous decrease from 4.5 to 3.0 ms, when T_S is increased from 50 to 200 °C.

Although r_H was maintained constant at 60%, the increase of T_S favours the incorporation of Si. Thus, when T_S is increased

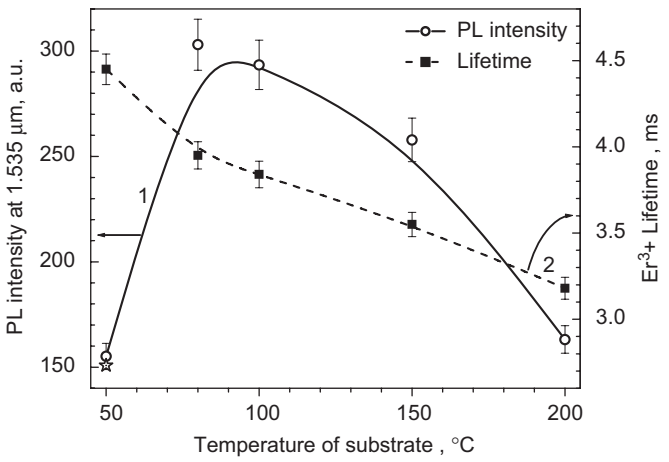

Fig. 2. Evolutions of the Er^{3+} PL intensity (curve 1) and lifetime (curve 2) recorded with the non-resonant excitation wavelength (476 nm) on the layers grown with $r_H = 60\%$, as a function of the substrate temperature T_S. The intensity of the reference sample is indicated by a star symbol.

from 100 to 200 °C, the Si excess was increased from 5 to 8 at%, while the Er content appears unaffected ($3.5–3.8 \times 10^{20}$ cm^{-3}). As already commented for the r_H effects, the smooth decrease of the lifetime is due to the T_S-induced smooth increase of Si excess. Note that our layers are still showing PL higher than the 'standard' sample described in Ref. [18], whose PL intensity is marked by a star symbol in Fig. 2.

3.3. Effect of annealing treatment

No Er^{3+} emission was observed from the as-deposited layers, while short (2 min) annealing at 800 °C results in the appearance of notable Er^{3+} emission (Fig. 3a). The increase of the annealing time from 2 to 60 min has led to double the PL intensity, while the lifetime increases from about 2.1 ms to nearly 5 ms. To mention that the annealing at the same temperature of the layers described in the previous sections leads to the following behaviours (data not shown): (i) the lifetime shows a higher value (about 3.5 ms) after 2 min annealing and increases steeply to a saturation value as high as 8.8 ms for 30 min treatment and (ii) the PL intensity reaches a maximum after 30 min annealing and then decreases slightly for longer treatment.

The structural changes induced by the thermal treatment have been analyzed through the evolution of the FTIR spectra. The short-time annealing leads to a sharp shift of TO_3 and LO_3 vibration bands towards the high-frequency side, indicating the occurrence of phase separation in the layers. Longer annealing resulted mainly in the increase of the intensity of the LO_3 band and the decrease of the TO_4–LO_4 doublet, suggesting an increase of the Si/SiO_2 interface area and an improvement of the oxide matrix, respectively.

The evolution of either the Er^{3+} PL intensity and lifetime with the annealing temperature T_a is displayed in Fig. 3b. This figure shows a gradual decrease of the PL intensity vs. T_a, while the lifetime increases rapidly to a saturation value of about 9 ms when T_a is increased to 800 °C.

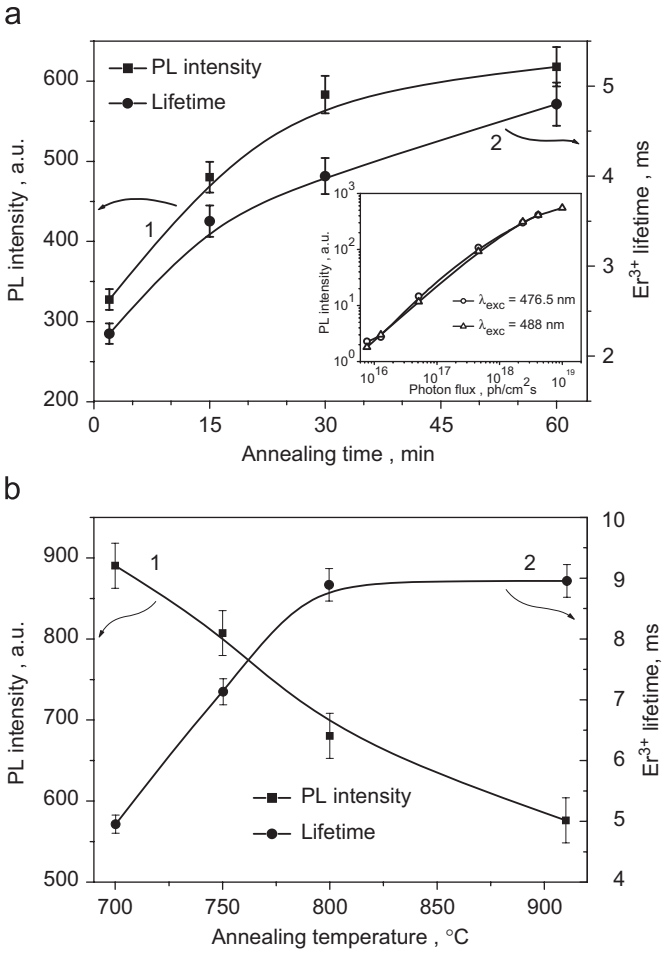

Fig. 3. (a) Variations of the Er^{3+} PL intensity (curve 1) and lifetime (curve 2) with the annealing duration. $T_a = 800$ °C. The inset compares the evolutions of the PL intensity against the photon flux for the two indicated excitation wavelengths, and for the layer annealed during 15 min. (b) Variations of the Er^{3+} PL intensity (curve 1) and lifetime (curve 2) towards the annealing temperature, using the same excitation conditions of (a) for the sample annealed during 60 min.

3.4. Analysis of the PL properties of the layer fabricated at optimal conditions

In this section, we will comment on the results obtained for the layers with the highest PL intensity that exceeds four times the one for the best "standard" layers described in Ref. [18]. Note that the present layers contain less Si excess (5 at% vs. 7 at%) and similar Er content ($\sim 3.5 \times 10^{20}$ at/cm^3). So, such efficiency could originate from the higher coupling rate between Si-nc and Er^{3+} ions.

The dependence of Er^{3+} PL intensity on photon flux was measured under non-resonant (476 nm) and resonant (488 nm) excitation to examine the coupling between Er^{3+} ions and Si clusters. From the inset of Fig. 3a, one can notice that the Er^{3+} emissions measured under the two excitation lines are comparable, while one expects higher Er PL under resonant excitation owing to the contribution of all optically active Er^{3+} ions (coupled and non-coupled to Si-nc).

We take into account that the Er^{3+} PL intensity at non-resonant excitation is proportional to $I_{PL}^{Er} \sim \sigma_{eff} \tau_{decay} N^*_{Er} \Phi / \tau_{rad}$, where σ_{eff} is the effective absorption cross-section, τ_{decay} is the measured lifetime, N^*_{Er} is the number of Er^{3+} ions coupled to Si-nc, Φ is the photon flux and τ_{rad} is the radiative lifetime. The τ_{decay} is ~6.3 ms for the layers investigated against 5 ms observed in Ref. [18], while the effective absorption cross-section, σ_{eff}, was found to be the same (4×10^{-17} cm^{-2}). The increase of τ_{decay} only could not explain the increase of PL intensity four times in the present layers. And hence we can assume that there is an increase of the fraction of Er ions coupled to Si-nc. The comparison of the PL intensities showed that the latter is about 11% of the total Er concentration instead of 3% reported for the former samples [18]. It is worth noting that such increase of the fraction of Er^{3+} ions coupled to Si-nc was also confirmed following the appropriate procedures described in Ref. [18]. However, in spite of promising results obtained in the present study, further improvement is needed to achieve a net gain in such layers.

4. Conclusions

In this paper, we have shown that the reactive co-sputtering of confocal targets allows the fabrication of SRSO-Er layers that show a significant enhancement of both Er^{3+} PL emission and Er^{3+} lifetime at 1.54 μm, in comparison with their counterparts for the best samples reported so far. The monitoring of the deposition and annealing conditions have enabled notable progress in the optimization of the material, leading to the increase of the fraction of coupled Er from a few % to about 11% with a lifetime reaching 8–9 ms. The observation of comparable Er^{3+} PL intensities under resonant and non-resonant excitations is indicative of the efficient sensitizing role of Si-nc towards the coupled Er ions, while the high lifetime would reflect the quality of both host matrix and surrounding of the Er ions. Finally, in spite of the

promising results, further improvements are necessary to obtain a net gain in the Er-coupled Si nanocluster material.

Acknowledgement

This work is supported by the European Community through the LANCER Project (FP6-IST 033574).

References

[1] A. Polman, J. Appl. Phys. 82 (1997) 1.
[2] F. Priolo, G. Franzò, S. Coffa, A. Carnera, Phys. Rev. B 57 (1998) 4443.
[3] W. Miniscalco, in: M. Digonnet (Ed.), Rare-Earth-Doped Fiber Lasers and Amplifiers, Dekker, New York, 2001, p. 62.
[4] A.J. Kenyon, P.F. Trwoga, M. Federighi, C.W. Pitt, J. Phys.: Condens. Matter 6 (1994) L319.
[5] M. Fujii, M. Yoshida, Y. Kansawa, S. Hayaski, K. Yamamoto, Appl. Phys. Lett. 71 (1997) 1198.
[6] J.H. Shin, K. Kim, S. Seo, C. Lee, Appl. Phys. Lett. 72 (1998) 1092.
[7] G. Franzò, V. Vinciguerra, F. Priolo, Appl. Phys. A: Mater. Sci. Process. 69 (1999) 3.
[8] M. Wodjak, M. Klik, M. Forcales, O.B. Gusev, T. Gregorkiewicz, L. Pacifici, G. Franzò, F. Priolo, F. Iacona, Phys. Rev. B 69 (2004) 233315.
[9] F. Gourbilleau, C. Dufour, M. Levalois, J. Vicens, R. Rizk, C. Sada, F. Enrichi, G. Battaglin, J. Appl. Phys. 94 (2003) 3869.
[10] K. Watanabe, M. Fujii, S. Hayashi, J. Appl. Phys. 90 (2001) 4761.
[11] F. Priolo, G. Franzò, D. Pacifici, V. Vinciguerra, F. Iacona, A. Irrera, J. Appl. Phys. 89 (2001) 264.
[12] D. Kovalev, J. Diener, H. Heckler, G. Polisski, N. Künzner, F. Koch, Phys. Rev. B 61 (2000) 4485.
[13] G. Franzò, S. Boninelli, D. Pacifici, F. Priolo, F. Iacona, C. Bongiorno, Appl. Phys. Lett. 82 (2003) 3871.
[14] F. Gourbilleau, L. Levalois, C. Dufour, J. Vicens, R. Rizk, J. Appl. Phys. 95 (2004) 3717.
[15] J.H. Jhe, J.H. Shin, K.J. Kim, D.W. Moon, Appl. Phys. Lett. 82 (2003) 4489.
[16] F. Gourbilleau, C. Dufour, R. Madelon, R. Rizk, J. Lumin. 126 (2007) 581.
[17] B. Garrido, C. Garcia, P. Pellegrino, D. Navarro-Urrios, N. Daldosso, L. Pavesi, F. Gourbilleau, R. Rizk, Appl. Phys. Lett. 89 (2006) 163103.
[18] B. Garrido, C. García, S.-Y. Seo, P. Pellegrino, D. Navarro-Urrios, N. Daldosso, L. Pavesi, F. Gourbilleau, R. Rizk, Phys. Rev. B 76 (2007) 245308.
[19] C. Ternon, F. Gourbilleau, X. Portier, P. Voivenel, C. Dufour, Thin Solid Films 419 (2002) 5.
[20] N. Tomozeiu, Appl. Surf. Sci. 25 (2006) 376.
[21] F. Gourbilleau, et al., Physica E, this issue.